Quantitative Confocal Spectral Imaging Analysis of Mitoxantrone Within Living K562 Cells: Intracellular Accumulation and Distribution of Monomers, Aggregates, Naphtoquinoxaline Metabolite, and Drug-Target Complexes

Alexei Feofanov,* Serguei Sharonov,# Fabrice Fleury,# Irina Kudelina,* and Igor Nabiev#
*Shemyakin and Ovchinnikov Institute of Bioorganic Chemistry, Russian Academy of Sciences, 117871 Moscow, Russia; and #Laboratoire de Spectroscopie Biomoléculaire, UFR de Pharmacie, Université de Reims Champagne-Ardenne, 51096 Reims Cedex, France

ABSTRACT Confocal spectral imaging (CSI) technique was used for quantitative analysis of the uptake, subcellular localization, and characteristics of localized binding and retention of anticancer agent mitoxantrone (MITOX) within human K562 erythroleukemia cells. The CSI technique enables identification of the state and interactions of the drug within the living cells. Utilizing this unique property of the method, intracellular distributions were examined for monomeric MITOX in polar environment, MITOX bound with hydrophobic cellular structures, naphthoquinoxaline metabolite, and nucleic acid-related complexes of MITOX. The features revealed were compared for the cells treated with 2 μM or 10 μM of MITOX for 1 h and correlated to the known data on antitumor action of the drug. MITOX was found to exhibit high tendency to self-aggregation within intracellular media. The aggregates are concluded to be a determinant of long-term intracellular retention of the drug and a source of persistent intracellular binding of MITOX. Considerable penetration of MITOX in the hydrophobic cytoskeleton structures as well as growing accumulation of MITOX bound to nucleic acids within the nucleus were found to occur in the cells treated with a high concentration of the drug. These effects may be among the factors stimulating and/or accompanying high-dose mitoxantrone-induced programmed cell death or apoptosis.

INTRODUCTION

Mitoxantrone (Novatrone™), a synthetic anthraquinone drug (for structure, see Feofanov et al., 1997b), shows considerable promise as an antitumor agent in treatment of acute nonlymphocytic leukemia, advanced breast cancer, and non-Hodgkin's lymphomas (Arlin et al., 1990; Ehninger et al., 1990; Faulds et al., 1991). A pharmacological effect of mitoxantrone (MITOX) is suggested to be closely related to its ability to bind with DNA. Few mechanisms of MITOX action involving formation of MITOX-DNA complexes have been proposed, including trapping of the topo II complex (Smith et al., 1990; D'Agra and Liu, 1989; Corbett and Osheroff, 1993) and aggregation and compaction of chromatin (Kapuscinski and Darzynkiewicz, 1986). It should be mentioned that topo II, a nuclear enzyme, is an essential part of a human cell's replication and transcription machinery (Wang, 1996). The recent results demonstrating that DNA topoisomerases are intracellular targets for a wide variety of known and emerging antitumor drugs appear to be among the most important discoveries in cancer research over the last three decades (Capranico and Zunino, 1995). The DNA-MITOX-topo II cleavable complex is a reversible molecular event, but it leads to cell death probably due to ongoing DNA-dependent processes, which may be the trigger of the cell death program.

Another type of DNA damage arises probably from formation of free radicals by MITOX (Basra et al., 1985). Besides DNA, MITOX binds to cytoplasmic structures (Roberts et al., 1989), and inhibition of microtubule assembly has been suggested to be a possible mechanism of the drug action at high concentrations (Ho et al., 1991).

Cytotoxicity of MITOX in HepG2 cells and in rat hepatocytes has been shown to be defined by the metabolites rather than by MITOX itself (Mewes et al., 1993). Since MITOX readily undergoes oxidation catalyzed by horseradish peroxidase (HRP) and cytochrome P-450 (Mewes et al., 1993; Reszka et al., 1986; Wolf et al., 1986), the cytotoxic action of the drug metabolites derived from oxidation by the cellular enzymes may appear as a general effect in other cells, particularly in the transformed human fibroblasts. Recently, a high concentration of MITOX (between 0.1 and 10 μM) was found to induce the programmed cell death (PCD) or apoptosis in leukemic cells (Bhalla et al., 1993). The data cited above demonstrate that a number of mechanisms can support antitumor activity of MITOX, and the

Received for publication 29 May 1997 and in final form 19 September 1997.

Address reprint requests to Prof. Igor Nabiev, Laboratoire de Spectroscopie Biomoléculaire, UFR de Pharmacie, Université de Reims Champagne-Ardenne, 51, rue Cognacq Jay, 51096 Reims, France. Tel.: 333-26053554; Fax: 333-26826001; E-mail: igor.nabiev@univ-reims.fr.

Abbreviations and trivial names used: mitoxantrone or MITOX, 1,4-dihydroxy-5,8-bis-{{[2-(2-hydroxyethyl)-amino]ethyl}amino}-9,10-anthracenedione dihydrochloride (NSC301739); $MITOX_{di}$, dimeric mitoxantrone; $MITOX_{mono}$, monomeric mitoxantrone located in polar environment; $MITOX_{NA}$, mitoxantrone bound with nucleic acids; $MITOX_{phob}$, mitoxantrone bound within the hydrophobic cellular structures; bp, base-pair; CSI, confocal spectral imaging; 2D, two-dimensional; 3D, three-dimensional; DMSO, dimethylsulfoxide; ds, double-stranded; FWHM, full width of spectrum at half of maximum; NQX, naphtoquinoxaline metabolite of mitoxantrone; PBS, phosphate buffered saline; topo II, DNA topoisomerase II.

0006-3495/97/12/3328/09 $2.00

relative contribution of each to the overall effect of the drug needs to be clarified at the different regimes of cell treatment with MITOX.

To shed light on roles of different mechanisms and biological targets in the pharmacological action of MITOX, the CSI technique was introduced to the noninvasive study of the drug uptake, distribution, and interactions in intact, viable cells (Sharonov et al., 1994; Feofanov et al., 1997b. The technique was shown to be complementary to conventional flow cytometry and laser scanning confocal fluorescence microscopy methods. The CSI technique is based on the analysis of a 2D set of spectra recorded from within drug-treated cells with ~0.5–1.5 μm^3 spatial resolution. It enables different states and interactions of the drug to be traced and mapped within the cell. The CSI technique allows intrinsic cellular fluorescence and enhancement/quenching of fluorescence of the drug localized in different states to be accounted for, and this is very important for correct quantitative analysis. Four different states of MITOX were identified and mapped within living K562 cells by means of the CSI technique (Feofanov et al., 1997b): $MITOX_{mono}$, $MITOX_{phob}$, $MITOX_{NA}$, and NQX metabolite (for structure, see Feofanov et al., 1997b).

This report describes the quantitative analysis of the uptake of MITOX in human K562 erythroleukemia cells exposed to 2 μM and 10 μM of MITOX for 1 h. Quantitative distributions of $MITOX_{mono}$, $MITOX_{phob}$, and $MITOX_{NA}$ and relative distributions of the intrinsic cellular fluorescence and NQX metabolite within intracellular compartments are mapped, and the sites of heterogeneous accumulation of the drug are characterized. Averaged intracellular concentrations and the patterns of intracellular distributions of $MITOX_{mono}$, $MITOX_{phob}$, and $MITOX_{NA}$ as a function of extracellular concentration of the drug are analyzed. Increased aggregation of MITOX within the cell in relation to aqueous buffer environment was observed. Accordingly, the majority of the drug molecules were found to accumulate in cytoplasmic compartments in an aggregated form. The features of localized binding and retention of MITOX observed by the CSI technique within human K562 erythroleukemia cells are correlated to the data on antitumor activity of the drug.

MATERIALS AND METHODS

Reagents and Cells

Stock solution (0.1 mM) of MITOX (Léderlé Laboratories, Rungis, France) was prepared in PBS. Concentration of MITOX in aqueous buffer solutions was measured by absorption at the isosbestic point at λ_i = 682 nm using extinction coefficient $\epsilon_{\lambda i} = 8.36 \times 10^3\ M^{-1}\ cm^{-1}$ (Kapuscinski et al., 1981). All other chemicals were of analytical-reagent grade and all solvents were of HPLC grade.

K562 is a human erythroleukemic cell line, established from a patient with chronic myelogeneous leukemia in blast transformation. The cells were grown exponentially at 3–7 $\times$ 10^5 cells/ml in RPMI-1640 (Gibco, Grand Island, NY) containing 10% fetal calf serum (Seromed) and 2 mM L-glutamine (Sigma).

The cells were incubated in the presence of 10^{-9}-10^{-6} M MITOX for 1 h. The cells were washed twice, resuspended with fresh media, and counted after mixing with 0.2% trypan blue. The IC_{50} was determined by plotting the number of viable cells as a percentage of the control against the drug concentration. All cytotoxicity assays were repeated three times. The drug IC_{50} was determined to be 30 ± 14 nM for the K562 cells.

To quantify the drug within the cells the DMSO extraction procedure was applied. After incubation with MITOX (10 μM of the drug for 1 h or 2 μM for 1 h) the cells (5 ml at 7 $\times$ 10^5 cells/ml) were rinsed two times with PBS and centrifuged at 180 $\times$ g for 5 min. The supernatant was removed and pellet was resuspended in 200 μl of DMSO for 20 min in order to extract MITOX. Afterward, the cells' homogenate was centrifuged at 180 $\times$ g for 5 min, and the drug-contained supernatant was collected. The concentration of the drug in supernatant was determined by absorption. Average intracellular concentration of the drug was calculated assuming the average diameter of cells to be 17 ± 3 μm. The average diameter of the cells was measured with a light microscope. For CSI measurements the cells treated with MITOX were rinsed twice with PBS, resuspended in the fresh PBS solution, and placed under the microscope.

Spectral measurements

Feofanov et al. (1997b) describe the instrumentation for CSI measurements as well as details of acquisition and treatment of spectral images. Each experimental spectrum recorded from a cell was decomposed as a sum of the reference spectra with appropriate coefficients. 2D maps of decomposition coefficients (hereafter referred to as spectral images) reflect relative distribution along the specimen of each component which spectrum was introduced as a reference.

Feofanov et al. (1997b) define the basic set of the reference spectra originated from in vitro modeling measurements. This set of spectra includes: (i) the spectrum of monomeric MITOX in aqueous environment; (ii) the spectrum of MITOX in propanol; (iii) the spectrum of MITOX-DNA complex; (iv) the spectrum of the NQX metabolite in dioxane; and (v) the spectrum of intrinsic cellular fluorescence. Spectrum (i) is assigned to $MITOX_{mono}$; spectrum (ii) is assigned to $MITOX_{phob}$; spectrum (iii) is considered to describe three types of complexes within the cells that cannot be spectrally distinguished, namely, MITOX-DNA complexes, ternary complexes between MITOX, DNA, and topo II, as well as ds $MITOX_{NA}$. Spectrum (iv) is assigned to the NQX metabolite bound to the acceptor groups of cellular structures or molecules.

Quantitative analysis of mitoxantrone intracellular concentration

The calibration procedures have been performed to estimate subcellular concentration of $MITOX_{mono}$, $MITOX_{phob}$, and $MITOX_{NA}$ based on intensity of the corresponding microfluorescence spectra. The spectra of monomeric MITOX in the aqueous buffer, MITOX in propanol and the spectra of the solution of MITOX-DNA complexes were measured as a function of the drug concentration under the microscope at the experimental conditions (lateral and axial resolution, laser power, amplitude of the scanning laser beam, integration time, etc.) used for recording the confocal spectral images. The calibration curves were obtained. To quantify the drug in these three states, a 2D set of the spectra measured from the cell was decomposed into components corresponding to the set of reference spectra, and fluorescence intensities of the corresponding components were recalculated into concentrations based on results of the calibration procedure.

As was shown previously, concentration-dependent formation of mitoxantrone dimers is accompanied by fluorescence quenching (Feofanov et al., 1997b). The amount of nonfluorescent $MITOX_{di}$ within the cells was estimated assuming that 1) the equilibrium constant of MITOX dimerization (K_d) in intracellular aqueous environment is the same as in aqueous buffer, and 2) the sites of intracellular accumulation of the monomeric and dimeric MITOX coincide. This estimation was based on the equation

$$[MITOX_{di}] = 2K_d \times [MITOX_{mono}]^2 \qquad (1)$$

where $[MITOX_{di}]$ is a concentration of MITOX molecules in dimeric state, $[MITOX_{mono}]$ is a concentration of monomeric MITOX, and $K_d = 3 \times 10^4$ m^{-1} (Kapuscinski and Darzynkiewicz, 1985).

The average concentrations of each component ($MITOX_{mono}$, $MITOX_{phob}$, $MITOX_{NA}$, and $MITOX_{di}$) within the cytoplasm and the nucleus of K562 cells were calculated basing on confocal spectral images measured at the equatorial optical section of the cells. To calculate the total average intracellular concentration of MITOX (C_{cell}) on the basis of CSI measurements, the equation

$$C_{cell} = C_{nuc}(V_{nuc}/V_{cell}) + C_{cyt}(V_{cyt}/V_{cell}) \quad (2)$$

is introduced, where C_{nuc} and C_{cyt} are the total average concentrations of MITOX in the nucleus and cytoplasm, respectively, including $MITOX_{mono}$, $MITOX_{phob}$, $MITOX_{NA}$, and $MITOX_{di}$ states; V_{nuc}, V_{cyt}, and V_{cell} are the volumes of nucleus, cytoplasmic region, and the cell as a whole, respectively. A relative volume of the nucleus (V_{nuc}/V_{cell}) was estimated by approximating the shapes of the cell and nucleus by spheres. Then

$$(V_{nuc}/V_{cell}) = (S_{nuc}/S_{cell})^{3/2} \quad (3)$$

and

$$(V_{cyt}/V_{cell}) = 1 - (S_{nuc}/S_{cell})^{3/2} \quad (4)$$

where S_{nuc} and S_{cell} are the areas of the nucleus and cell, respectively, at the equatorial section. These areas were measured using recorded spectral images, and, finally, C_{cell} was calculated for each scanned cell as

$$C_{cell} = C_{nuc}(S_{nuc}/S_{cell})^{3/2} + C_{cyt}[1 - (S_{nuc}/S_{cell})^{3/2}] \quad (5)$$

Assuming that 1) the cells attached to the plastic change from a spherical shape to an ellipsoidal one with the axis c_z less than $a_x = b_y$, and 2) the cell and its nucleus undergo similar attachment-induced deformation (the ratios c_z/a_x for the cell as a whole and for the nucleus are equal), we come up with exactly the same Eq. 5.

It should be mentioned that like many other cells, the K562 cells tend to adopt the quasispherical shape in suspension. SCI measurements were performed during the next 10–20 min after the cells were resuspended (see Experimental section). Obviously, the cells just resuspended were not so tightly attached on the plastic to sprawl and to change considerably initially spherical or ellipsoidal shape. As examined with the optical microscope, the freshly attached K562 cells have circular cross-sections ($a_x = b_y$) and the average diameter of the attached cells is increased only slightly as compared with the cells in suspension (small attachment-induced deformation). Therefore, our assumption on the shape of the cell appears reasonable in estimating intracellular concentration of MITOX.

Averaged over 30 cells, the area of nucleus at the equatorial section was measured to be 43 ± 9% of the cell area. Assuming the shapes of both cell and nucleus are spherical (or ellipsoidal), the volume of nucleus was estimated to be 28 ± 9% of the cell volume.

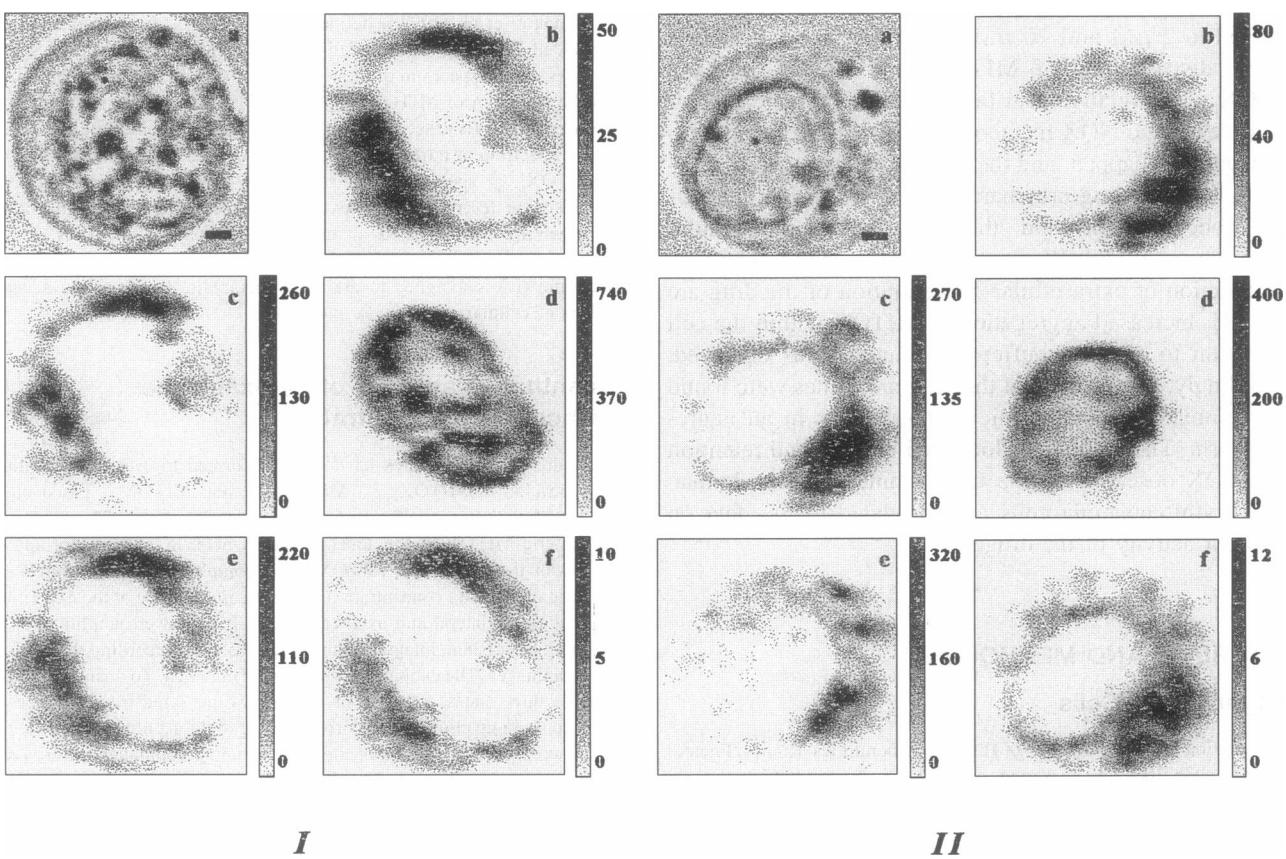

FIGURE 1. Confocal spectral images of two typical cells (*I* and *II*) exposed to 10 μM MITOX for 1 h. Conventional light-microscope image of the cell (*a*). Localization of intrinsic cellular fluorescence (*b*). Spectral images describing the subcellular distribution of monomeric MITOX in the polar environment (*c*), nucleic acid related complexes of MITOX (*d*), MITOX bound within hydrophobic cellular structures (*e*) as well as NQX metabolite bound to the ligands (*f*). Scales are independent of each other and show the concentration of MITOX in μM for the images (*c*, *d*, *e*) as well as the relative intensity of signal in arbitrary units for the images (*b*, *f*). Bar shown on the image (*a*) corresponds to 2 μm.

RESULTS

Localization, state, and interactions of mitoxantrone in the K562 cells

Confocal spectral images of cells after exposure to 10 μM of MITOX for 1 h as well as cells after treatment with 2 μM MITOX for 1 h are shown in Figs. 1 and 2, respectively. These images describe 2D quantitative distribution of monomeric MITOX in $MITOX_{mono}$, $MITOX_{phob}$, $MITOX_{NA}$, and relative distribution of the NQX metabolite and intrinsic fluorescence of the cells along the equatorial optical section.

According to our previous study (Feofanov et al., 1997b), $MITOX_{mono}$ is the monomeric drug molecules localized in a polar (aqueouslike) intracellular environment. They may be either free or bound through the alkylamino side chains to cellular molecules. Such interactions, which involve the side chains but not the chromophore moiety of MITOX, do not affect fluorescence of the drug and thereby cannot be discriminated. $MITOX_{phob}$ is the drug molecules involved in forced hydrophobic contacts and/or the molecules having the chromophore moiety in a nonpolar environment due to binding of the drug within the hydrophobic cellular structures. $MITOX_{NA}$ is referred to as the molecules bound with ds fragments of RNA, ds DNA alone, or within ternary complexes between MITOX, DNA, and topo II. These three types of complexes are characterized by a similar mode of interaction; that is, intercalation of the MITOX chromophore in ds helix of DNA or RNA, and, showing similar fluorescence spectra, cannot be spectrally distinguished within the cells. The features of fluorescence of the NQX metabolite in a cellular environment indicate that it is bound to the acceptor groups of cellular molecules (Feofanov et al., 1997b). The parameters of the reference spectra corresponding to $MITOX_{mono}$, $MITOX_{phob}$, $MITOX_{NA}$, and bound NQX metabolite are listed in Table 1.

MITOX undergoes concentration-dependent formation of dimers (Kapuscinski and Darzynkiewicz, 1985). Dimeric MITOX does not fluoresce (Feofanov et al., 1997b) and cannot be measured in cells by CSI. Nevertheless, due to an inherent property of MITOX to aggregate, it is reasonable to suggest that dimeric MITOX is co-distributed with free $MITOX_{mono}$ within the cell.

Distributions of MITOX and its complexes are quite heterogeneous within the cell. $MITOX_{mono}$, $MITOX_{phob}$,

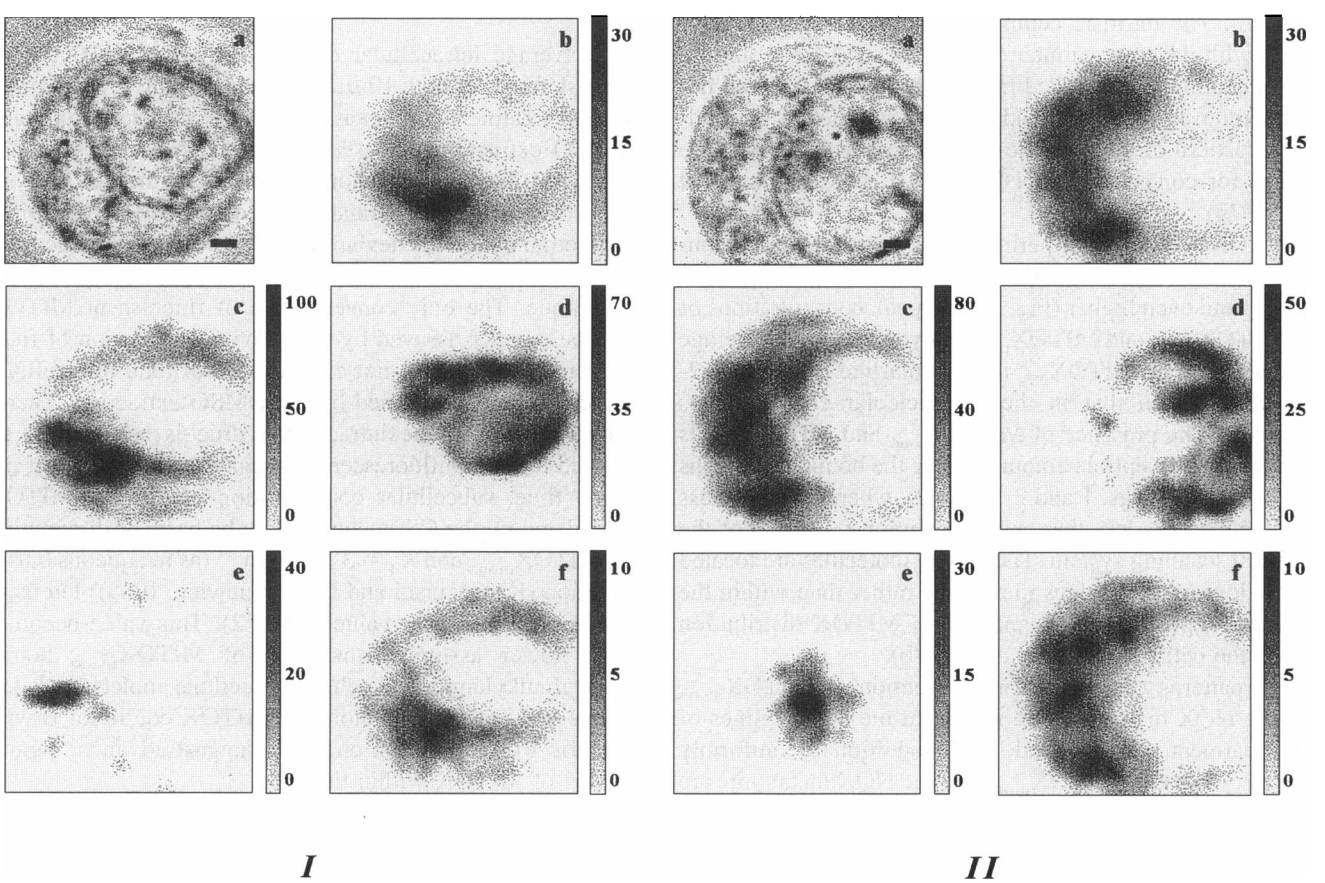

FIGURE 2. Confocal spectral images of the two typical cells (*I* and *II*) exposed to 2 μM MITOX for 1 h. Conventional light-microscope image of the cell (*a*). Localization of intrinsic cellular fluorescence (*b*). Spectral images describing subcellular distribution of monomeric MITOX in the polar environment (*c*), nucleic acid related complexes of MITOX (*d*), MITOX bound within hydrophobic cellular structures (*e*) as well as NQX metabolite bound to the ligands (*f*). Scales are independent of each other and show the concentration of MITOX in μM for the images (*c*, *d*, *e*) as well as the relative intensity of signal in arbitrary units for the images (*b*, *f*). Bar shown on the image (*a*) corresponds to 2 μm.

TABLE 1 Spectral parameters of the absorption and fluorescence spectra used as models for the analysis of interactions of mitoxantrone and its naphtoquinoxaline metabolite in the K562 cells

	Absorption			Fluorescence*		
Models	λ_{max1} (nm)	λ_{max2} (nm)	R_A#	λ_{max} (nm)	FWHM§ (nm)	I_{rel}¶
‖$MITOX_{mono}$	610	661	1.34	685	58	1.0
**$MITOX_{phob}$	623	675	1.34	694	46	2.1
##$MITOX_{NA}$	628	680	1.34	700	50	0.65
§§Bound NQX	588	636	1.2	652	36	

*Intensities were corrected for the effect of inner filter. Excitation wavelength, 514.5 nm.
#Ratio of absorbance at λ_{max2} to that at λ_{max1}.
§Full width of spectrum at the half of maximum.
¶Relative intensity as compared with the intensity of equimolar aqueous solution of monomeric MITOX.
‖Monomeric MITOX in polar intracellular environment.
**MITOX bound within hydrophobic cellular structures.
##MITOX-DNA, MITOX-DNA-topo II, and MITOX-RNA complexes.
§§NQX metabolite of MITOX bound with acceptor groups of molecules in the cell.

and NQX metabolite accumulate in cytoplasm, whereas $MITOX_{NA}$ dominates within the nucleus (Figs. 1 and 2; Table 2). The intrinsic cellular fluorescence intensity also varies with different cellular compartments (Figs. 1 and 2). It is exceptionally observed from within cytoplasm and has a maximum in the regions adjacent to the nucleus. A qualitative pattern of the intrinsic fluorescence was found to be similar for control and MITOX-treated cells (Feofanov et al., 1997b).

$MITOX_{NA}$ stains the perinucleolar region and accumulates in nucleolarlike bodies at concentrations comparable (Fig. 1) and even higher (Fig. 2) than peak concentrations of the $MITOX_{mono}$ and $MITOX_{phob}$ in cytoplasm. The average concentration of $MITOX_{NA}$ in nucleolarlike bodies is ~2-fold higher than that in the perinucleolar compartments (Table 2). The presence of $MITOX_{mono}$ and $MITOX_{phob}$ is observed in perceptible amounts along the boundary regions of the nucleus (Figs. 1 and 2; Table 2), where the thickness of the nucleus is less than axial resolution (~3 μm) of the confocal scanning system. These drug molecules are located on or close to the nucleus membrane rather than within the nucleus, as proved by 3D analysis of MITOX distribution within the cell (Feofanov et al., 1997b).

The patterns of subcellular distribution of $MITOX_{mono}$ and the NQX metabolite are similar at the both regimes of cell treatment (Figs. 1 and 2). In addition to uniformly stained cytoplasm, $MITOX_{mono}$ and the NQX metabolite are accumulated in a compact region adjacent to the nucleus. The peak concentrations of $MITOX_{mono}$ observed in this region are ~2.5-fold higher than in the peripheral cytoplasm. The regions of concentrated $MITOX_{mono}$ and the NQX metabolite coincide with the sites of intense intrinsic fluorescence of the cell (Figs. 1 and 2).

It should be mentioned that the NQX metabolite fluoresces much more intensely as compared to an equimolar solution of MITOX at the 514.5 nm excitation used for CSI measurements. Since the NQX metabolite hardly contributes to an overall intracellular fluorescent signal (Feofanov et al., 1997b), its concentration in the cells is inferred to be rather small. Therefore, we do not perform quantitative analysis here and report only on relative distribution of the NQX metabolite in the cells.

The pattern of $MITOX_{phob}$ distribution was found to differ from the patterns observed for both $MITOX_{mono}$ and the NQX metabolite, and it depends on the drug concentration used to treat the cells. $MITOX_{phob}$ is enfolded in small cytoplasmic inclusions (Fig. 2, *Ie*) which tend to group close to the nucleus (Fig. 2, *IIe*) in the cells exposed to 2 μM of MITOX. In opposite, besides small inclusions of $MITOX_{phob}$, general staining of hydrophobic cellular structures appears in the cytoplasm of the cells treated with 10 μM of the drug (Fig. 1, *Ie*, *IIe*). It is noteworthy that we have not attempted yet to identify the origin of either of these inclusions or stained hydrophobic cellular structures at the present stage of the study.

Concentration-dependent accumulation and distribution of mitoxantrone in the cells

The average intracellular concentrations of MITOX have been defined for both 10 μm × 1 h and 2 μm × 1 h regimes of cell treatment by means of both the CSI technique and DMSO extraction as described in Materials and Methods (Table 3). The concentrations calculated by the CSI analysis are obviously underestimated as compared to the DMSO extraction data. This deviation is likely due to intrinsic error in estimating concentration of dimeric MITOX by the CSI technique. The only concentration of fluorescent MITOX can be directly assayed by CSI. The concentration of fluorescent MITOX does not exceed 30% of total intracellular concentration determined by the DMSO extraction. Therefore, the rest of the intracellular drug is assumed to be related to the nonfluorescent aggregates of MITOX. At the same time, subcellular concentration of dimeric MITOX calculated by the CSI technique on the basis of distribution of $MITOX_{mono}$ and $K_d = 3 \times 10^4$ m^{-1} (as in aqueous buffer solution (Kapuscinski and Darzynkiewicz, 1985)) led us to a considerably lower value (Table 2). This value becomes even lower assuming that part of $MITOX_{mono}$ bound through alkylamino side chains to cellular molecules is not concerned with free monomeric MITOX equilibrated with dimeric MITOX. Thus, one may suggest advanced aggregation of MITOX within the cells.

Finally, combining the results obtained by the DMSO extraction with the CSI analysis data it can be concluded that ~70% of intracellular MITOX is accumulated in the cytoplasmic region in the aggregated form. The cellular uptake of MITOX is very high, exceeding ~80-fold the extracellular concentration of the drug and does not exhibit a saturation even at the 10 μM × 1 h regime of cell treatment.

TABLE 2 Average subcellular concentration of mitoxantrone (mean ± SE) in different states and complexes in K-562 cells as estimated by confocal spectral imaging analysis

State of Mitoxantrone in the Cells	10 μM × 1 h Dose of Treatment				2 μM × 1 h Dose of Treatment			
	Average Concentration of Mitoxantrone				Average Concentration of Mitoxantrone			
	Cytoplasm (μM)	Nucleus (μM)	Nucleoli (μM)	Perinucleolar region (μM)	Cytoplasm (μM)	Nucleus (μM)	Nucleoli (μM)	Perinucleolar region (μM)
MITOX-DNA*	11 ± 7	270 ± 170	410 ± 150	203 ± 135	2.1 ± 1.5	45 ± 24	64 ± 21	35 ± 18
$MITOX_{phob}$#	54 ± 36	31 ± 22			2.9 ± 1.7	4 ± 2		
$MITOX_{mono}$§	75 ± 47	22 ± 12			23 ± 14	13 ± 6		
$MITOX_{dimer}$¶	352 ± 280	44 ± 26			43 ± 21	16 ± 12		

*MITOX-DNA, MITOX-DNA-topo II, and MITOX-RNA complexes.
#MITOX bound within hydrophobic cellular structures.
§Monomeric MITOX in polar intracellular environment.
¶Dimers of MITOX. It was calculated from distribution of monomeric MITOX assuming the equilibrium constant of dimerization $K_d = 3 \times 10^4\ M^{-1}$ (Kapuscinski and Darzynkiewicz, 1985).

The relative concentrations of $MITOX_{NA}$ in the nucleus are 0.34 and 0.28 of average intracellular concentrations at the 10 μm × 1 h and 2 μm × 1 h treatments, respectively. So, MITOX penetrates in the nucleus and complexes with nucleic acids proportionally to extracellular concentration of the drug. The absence of saturation even at the 10 μm × 1 h cell treatment is typical for this process. Preferential, ~2-fold higher, localization of $MITOX_{NA}$ within the nucleoli as compared to the perinucleolar region is retained at both 2 μM and 10 μM extracellular concentrations of MITOX (Table 2).

Relative cytoplasmic concentrations of $MITOX_{phob}$ are equal to 0.07 and 0.02 of average intracellular concentrations at the 10 μm × 1 h and 2 μm × 1 h treatments, respectively. The concentrations of $MITOX_{phob}$ and $MITOX_{mono}$ become comparable (Table 2), and general staining of hydrophobic cellular structures appears (Fig. 1) at the 10 μm extracellular concentration of MITOX. It clearly indicates concentration-dependent enhancement of the drug penetration in and/or binding within hydrophobic cellular structures. No such an effect in respect to the cellular membrane is distinctly observed. At the same conditions relative cytoplasmic concentration of $MITOX_{mono}$ falls from 0.14 to 0.095 of average intracellular concentrations, demonstrating moderate concentration-dependent saturation. This saturation occurs probably due to both more strong capture of the drug in hydrophobic structures and enhanced aggregation of MITOX within the cells exposed to 10 μM of the drug.

TABLE 3 Intracellular concentration of mitoxantrone calculated on the basis of CSI analysis (mean ± SE) and measured by DMSO extraction for two regimes of cell treatment by the drug

Dose of Treatment	Intracellular Concentration of the Drug (μM) According to	
	CSI Analysis	DMSO Extraction
10 μM for 1 h	456 ± 240	790 ± 360
2 μM for 1 h	72 ± 38	162 ± 75

DISCUSSION

The quantitative analysis of uptake and distribution of MITOX within the K562 cells was performed by utilizing the unique ability of CSI technique to characterize state and interactions of MITOX within intact, living cells. The goal of the study is to find an approach to clarify relative contributions of different mechanisms of antitumor action reported for MITOX. In this way we are going to combine conventional biochemical and cytological methods with noninvasive quantitative CSI analysis. As the first step we attempt to characterize by CSI technique the features of MITOX interactions and distribution within living K562 cells in order to find correlation with known biochemical data on accumulation and activity of MITOX in cancer cells.

Features of mitoxantrone accumulation within the cells

The quantitative CSI analysis combined with the DMSO extraction procedure shows that intracellular MITOX concentration exceeds ~80-fold its extracellular concentration in the human erythroleukemic K562 cells exposed to 2 μM and 10 μM of MITOX for 1 h (Table 3). Appearance of the drug within different cellular compartments was observed during the first 20 min of incubation, demonstrating fast cellular uptake of MITOX. In contrast, the active efflux of MITOX was found to be less efficient.

These findings are in general accordance with the data on dynamics of the cellular uptake of MITOX. Intracellular concentration of the drug exceeded ~240-fold the extracellular one when the human colon carcinoma WiDr cells were exposed to 1.9 μM of MITOX for 1 h (Wallace et al., 1987). Appearance of the drug within different cellular compartments of the WiDr cells (Roberts et al., 1989) and SV40

transformed human MRC5CVI fibroblasts (Smith et al., 1992) was observed at the same time scale as for the K562 cells. Long-term intracellular retention of MITOX was reported for the WiDr cells (Roberts et al., 1989; Wallace et al., 1987), MRC5CVI cells (Smith et al., 1992; Fox and Smith, 1990) and for 1Br3gn2, GM0637, AT5BIVA, NE1–3/48 cells (Fox and Smith, 1990). The drug retention was suggested to be an important determinant of the MITOX action resulting in G_2 cell cycle arrest and cellular damage.

In this study the drug was revealed to accumulate heterogeneously within cytoplasm in the forms of monomeric MITOX exposed to polar intracellular environment, MITOX bound within hydrophobic cellular structures, and aggregated MITOX. Metabolization of MITOX results in formation of the NQX metabolite. $MITOX_{mono}$ is a free drug or drug bound through alkylamino side chains to cellular molecules. Its relative concentrations in cytoplasm are 0.095 and 0.14 of the average intracellular concentrations at the 10 μM × 1 h and 2 μM × 1 h cell treatments, respectively. The relative concentrations of $MITOX_{phob}$ in cytoplasm are equal to 0.07 and 0.02 at the 10 μM × 1 h and 2 μM × 1 h cell treatments, respectively.

The aggregation of MITOX was concluded to increase in an intracellular medium as compared to an aqueous buffer environment, and the majority (~70%) of the accumulated drug was found to be aggregated. This intracellular aggregated drug is not directly involved in the drug-target interactions, but on dissociation the aggregates can be a source for continually reforming the drug-target complexes. One may suppose that long-term inhibition of DNA synthesis and persistence of the trapped topo II complexes (Fox and Smith, 1990) result (at least partially) from long-term maintenance of the cytotoxic concentration of MITOX due to slow dissociation of aggregates in response to the efflux of the monomeric drug. This conclusion is also confirmed by the data of a biochemical fractionation procedure (Roberts et al., 1989) which revealed that 1) a principal part of MITOX in the cells exposed to 50 μM for 1 h is associated with the cytoplasmic fraction, and 2) further incubation (up to 72 h) of cells in a drug-free medium is accompanied by a decrease in the relative amount of MITOX in the cytoplasmic fraction, while the drug content in the fraction enriched by DNA and RNA relatively increases.

The CSI analysis revealed that accumulation of MITOX within the nucleus occurs 1) proportionally to the extracellular concentration of the drug, 2) at the average concentration ~24-fold exceeding its extracellular value, 3) at ~2-fold higher concentration in the nucleoli than in the nucleoplasm, 4) without saturation up to 10 μM for 1 h dosage of cell treatment, and 5) predominantly in the form of the drug complexes with ds nucleic acids.

The origin of intrinsic cellular fluorescence and preliminary assignments of the sites of cytoplasmic localization of mitoxantrone

While more detailed studies based on simultaneous treatment of cells with MITOX and selective labeling of cellular organelles will be the subject of a separate publication, we discuss here preliminary assignments of the sites of cytoplasmic localization of the drug.

The spectra of intrinsic fluorescence of the K562 cells excited at 514.5 nm are quite broad. They exhibit two overlapped maxima at 640 and 652 nm and a shoulder at ~700 nm (Feofanov et al., 1997b). The cellular fluorescence in the red was shown to correspond to porphyrins (Udenfreid, 1965; Gurinovich et al., 1968; Maneshin and Arevshatian, 1972). Luminescence features of different porphyrins (copro, uro, meso, aetio, and hematoporphyrins) are very similar: major band, 625 nm; γ, 654 nm; β, 673 nm; α, 691 nm (Udenfreid, 1965). The fluorescence spectrum of protoporphyrin IX has maxima at 635 nm and 703 nm and strongly depends on environmental conditions (Gurinovich et al., 1968). On adding glycerin to the ethanol solution of protoporphyrin a new band appears at 676 nm, whereas intensity of the 635 nm band decreases and the 703 nm band becomes a weak shoulder (Gurinovich et al., 1968). Evidently, overlapping of the signals of several porphyrins located in different microenvironments determines the spectra observed from the K562 cells. Accumulation of porphyrins in the cells was assigned to functioning of the enzymes of respiratory chain involved in the transfer of electrons (Maneshin and Arevshatian, 1972). Mitochondria are believed to be the principal sites of porphyrin accumulation. Therefore, intrinsic fluorescence of cells in the red region may be considered as a natural fluorescent marker of mitochondria.

The results of the CSI analysis show that the regions of concentrated $MITOX_{mono}$ and NQX metabolite coincide with the sites of intense intrinsic cellular fluorescence (Figs. 1 and 2). Though the resolution achieved is not enough to assert if the drug and its metabolite are localized within mitochondria, at least the proximity of the sites of both preferential accumulation of the drug and its metabolization to the mitochondrial system seem to be obvious. In accordance with the data published before (Wolf et al., 1986; Blanz et al., 1991; Kolodziejczyk et al., 1988) one may conclude that the NQX metabolite originates from oxidative action of cellular enzymes. As revealed by CSI analysis, it is bound to the acceptor groups of some ligands within the cells.

Considerable accumulation of MITOX (up to 7%) accompanied by pronounced change in the pattern of its distribution was detected within hydrophobic cytoplasmic cellular structures by the CSI technique when extracellular drug concentration increased from 2 to 10 μM (Tables 2 and 3). Previously, by using the biochemical fractionation procedure, ~10% of the persistent drug binding was found to be associated with water insoluble cytoskeleton fraction within the WiDr cells (Roberts et al., 1989). Cytokeratin and lamin intermediate filaments were identified as dominant proteins in the cytoskeleton fraction. It has been also reported (Ho et al., 1991) that MITOX plays a role of a microtubule inhibitory agent and can exert its intracellular effect through modulation of microtubule assembly. Poly-

merization of tubulin was found to be inhibited in the presence of 2 to 10 μM of MITOX in proportion to dosage. Each time when the effect of MITOX on hydrophobic proteins and/or cellular structures was observed, the cells were exposed to high concentrations of MITOX: 2–10 μM (Ho et al., 1991), and 50 μM (Roberts et al., 1989). Therefore, one may assume that concentration-dependent changes in the pattern of accumulation and distribution of $MITOX_{phob}$ observed by the CSI technique manifest the appearance of MITOX binding within hydrophobic, most probably cytoskeleton, structures of the cells.

Interactions of mitoxantrone with nucleic acids in nucleus

Our previous results (Feofanov et al., 1997b) imply that MITOX binds to ds nucleic acids by intercalation within the nucleus. At the same time, the antitumor activity of MITOX is suggested to be related to inhibition of topo II by stabilization of the topo II-DNA cleavable complex (Smith et al., 1990; D'Agra and Liu, 1989; Corbett and Osheroff, 1993) as well as to the compaction and aggregation of chromatin (Kapuscinski and Darzynkiewicz, 1986) rather than to DNA intercalation itself. In our experiments the cells were treated by MITOX in the logarithmic phase of the cell growth, in which the expression and activity of the α-isoform of topo II are the highest (Zini et al., 1994). It is known that the 170-kDa α-isoform of topo II is presumably distributed in the perinucleolar region and at ~2-fold lower density in the nucleoli of K562 cells, whereas the 180-kDa β-isoform of topo II is exclusively present in the nucleoli (Zini et al., 1994). Therefore, some part of the MITOX-DNA complexes detected by the CSI analysis should be involved in formation of the ternary cleavable topo II-MITOX-DNA complexes. These ternary complexes cannot be distinguished from binary MITOX-DNA complexes by spectral fluorescence analysis, because their spectral parameters are identical (Feofanov et al., 1997b). The relative amount of the drug involved in the ternary cleavable complexes is rather small as compared to the total amount of MITOX bound with nucleic acids. It follows from the fact that relatively low intranuclear concentration of MITOX results in topo II-related DNA damage (Smith et al., 1992). Moreover, the formation of the ternary cleavable complexes reaches saturation at 1.25–2.5 μM extracellular concentrations of the drug.

Our experiments reveal that amount of the drug bound to nucleic acids continues to grow in cell nucleus without saturation even when the cells are exposed to 10 μM of MITOX (Table 2). It exceeds considerably the concentration when the formation of ternary cleavable complexes is saturated. The continuous accumulation of $MITOX_{NA}$ has to be accompanied by a dramatic increase in a drug/bp ratio for intranuclear MITOX-DNA complexes and to result in macro-destruction of nucleic acid conformation. From our in vitro experiments (Feofanov et al., 1997b), unwinding of the DNA helix has been shown to accompany binding of MITOX to DNA, when the drug/bp molar ratio increases from 1:100 to 1:5, eventually resulting in precipitation of the drug-DNA complexes. Compaction and aggregation of nuclear chromatin was observed by electronic microscopy in the L1210 cells treated with MITOX (Kapuscinski and Darzynkiewicz, 1986). In this sense, the evidence that high-dose mitoxantrone induces programmed cell death or apoptosis (Bhalla et al., 1993) appears to be directly concerned with the ability of MITOX to be accumulated thoroughly in nuclear complexes with nucleic acids. MITOX-related disruption of the native structure of nucleic acids may activate nuclear endonuclease and lead to fragmentation of genomic DNA being a characteristic feature for apoptosis.

At present it is not clear whether advanced binding of MITOX with hydrophobic cellular structures observed at high drug concentrations is also associated to apoptosis activation or it manifests appearance of additional drug targets independent from apoptosis. In both cases the alteration of the structure and/or normal functioning of cellular cytoskeleton is speculated.

At high extracellular concentrations MITOX heavily accumulates within cancer cells, especially within the nucleus in the form of complexes with nucleic acids. It predetermines induction of additional mechanisms of cell killing, in particular, apoptosis, which is sometimes more important than inhibition of topo II. It is presumed to be very useful to overcome cellular resistance to MITOX when it is originated from a low level of topo II or expression of mutant topo II resistant to the drug. It is known that plasma concentrations of MITOX achieve a level from 1 to 10 μm (Ehninger et al., 1986), and high-dose drug regimes have significant clinical activity in leukemias (Arlin et al., 1990; Ehninger et al., 1986).

We are grateful to A. Kokota for excellent software assistance and to H. Morjani for assistance with cell manipulations. We also thank all the people that helped us at the DILOR S.A. (Lille, France). We are particularly grateful to M. Manfait for providing stimulating discussions during the course of this study and manuscript preparation. We thank E. Kryukov for critical reading of the manuscript and English correction.

This research was supported by Grant 96-04-48421 from the Russian Foundation for Basic Research and Grant 1379 from the Association pour la Recherche Contre le Cancer (France). A.F. was supported by a FEBS short-term fellowship.

REFERENCES

Arlin, Z., D. C. Case, J. Moore, P. Wiernik, E. Feldman, S. Saletan, P. Desai, L. Sia, and K. Cartwright. 1990. Lederle cooperative group: randomized multicenter trial of cytosine arabinoside with mitoxantrone or daunorubicin in previously untreated adult patients with acute nonlymphocytic leukemia (ANLL). *Leukemia.* 4:177–184.

Basra, J., C. R. Wolf, J. R. Brown, and L. H. Patterson. 1985. Evidence for human liver mediated free-radical formation by doxorubicin and mitoxantrone. *Anticancer Drug Design.* 1:45–52.

Bhalla, K., A. M. Ibrado, E. Tourkina, C. Tang, S. Grant, G. Bullock, Y. Huang, V. Ponnathpur, and M. E. Mahoney. 1993. High-dose mitoxantrone induces programmed cell death or apoptosis in human myeloid leukemia cells. *Blood.* 82:3133–3140.

Blanz, J., K. Mewes, G. Ehninger, B. Proksch, D. Waidelich, B. Greger, and K.-P. Zeller. 1991. Evidence for oxidative activation of mitoxantrone in human, pig and rat. *Drug Metab. Dispos.* 19:871–880.

Capranico, G., and F. Zunino. 1995. Antitumor inhibitors of DNA topoisomerases. *Current Pharmaceutical Design.* 1:1–14.

Corbett, A. H., and N. Osheroff. 1993. When good enzymes go bad: conversion of topoisomerase II to a cellular toxin by antineoplastic drugs. *Chem. Res. Toxicol.* 6:586–597.

D'Agra, P., and L. F. Liu. 1989. Topoisomerase-targeting antitumor drugs. *Biochim. Biophys. Acta.* 989:163–177.

Ehninger, G., B. Proksch, G. Heinzel, and D. L. Woodward. 1986. Clinical pharmacology of mitoxantrone. *Cancer Treat Rep.* 70:1373–1379.

Ehninger, G., U. Schuler, B. Proksch, K.-P. Zeller, and J. Blanz. 1990. Pharmacokinetics and metabolism of mitoxantrone. A review. *Clin. Pharmacokinet.* 18:365–380.

Faulds, D., J. A. Balfour, P. Chrisp, and H. D. Langtry. 1991. Mitoxantrone. A review of its pharmacodynamic and pharmacokinetic properties, and therapeutic potential in the chemotherapy of cancer. *Drugs.* 41:400–449.

Feofanov, A., S. Sharonov, I. Kudelina, F. Fleury, and I. Nabiev. 1997. Localization and molecular interactions of mitoxantrone within living K562 cells as probed by confocal spectral imaging analysis. *Biophys. J.* 73:3317–3327.

Fox, M. E., and P. J. Smith. 1990. Long-term inhibition of DNA synthesis and the persistence of trapped topoisomerase II complexes in determining the toxicity of the antitumor DNA intercalators mAMSA and mitoxantrone. *Cancer Res.* 50:5813–5818.

Gurinovich, G. P., A. H. Sevchenko, and K. H. Solovyev. 1968. Spectroscopy of chlorophyll and related compounds. Nauka i Technika, Minsk.

Ho, C. K., S. L. Law, H. Chiang, M. L. Hsu, C. C. Wang, and S. Y. Wang. 1991. Inhibition of microtubule assembly is a possible mechanism of action of mitoxantrone. *Biochem. Biophys. Res. Commun.* 180:118–123.

Kapuscinski, J., and Z. Darzynkiewicz. 1985. Interactions of antitumor agents ametatrone and mitoxantrone (Novatrone) with double-stranded DNA. *Clin. Pharmacol.* 34:4203–4213.

Kapuscinski, J., and Z. Darzynkiewicz. 1986. Relationship between the pharmacological activity of the antitumor drugs ametantrone and mitoxantrone and their ability to condense nucleic acids. *Proc. Natl. Acad. Sci. USA.* 83:6302–6306.

Kapuscinski, J., Z. Darzynkiewicz, F. Traganos, and M. R. Melamed. 1981. Interaction of a new antitumor agent, 1–4-dihydroxy-5,8-bis-[[2-(2-hydroxyethyl)-amino]ethyl]amino]-9,10-anthracenedione, with nucleic acids. *Biochem. Pharmacol.* 30:231–240.

Kolodziejczyk, P., K. Reszka, and J. W. Lown. 1988. Enzymatic oxidative activation and transformation of the antitumor agent mitoxantrone. *Free Radicals Biol. & Med.* 5:13–25.

Maneshin, S. K., and A. A. Arevshatian. 1972. On the question of porphyrin luminescence in the cells of Candida yeast. *Biophysika.* 17: 352–354.

Mewes, K., J. Blanz, G. Ehninger, R. Gebhard, and K.-P. Zeller. 1993. Cytochrome P-450-induced cytotoxicity of mitoxantrone by formation of electrophilic intermediates. *Cancer Res.* 53:5135–5142.

Reszka, K., P. Kolodziejczyk, and J. W. Lown. 1986. Horseradish peroxidase-catalyzed oxidation of mitoxantrone: spectrophotometric and electron paramagnetic resonance studies. *J. Free Rad. Biol. Med.* 2:25–32.

Roberts, R. A., A. E. Cress, and W. S. Dalton. 1989. Persistent intracellular binding of mitoxantrone in a human colon carcinoma cell line. *Biochem. Pharmacol.* 38:4283–4290.

Sharonov, S., I. Chourpa, H. Morjani, I. Nabiev, M. Manfait, and A. Feofanov. 1994. Confocal spectral imaging analysis in studies of the spatial distribution of antitumor drugs within living cancer cells. *Anal. Chim. Acta.* 290:40–47.

Smith, P. J., S. A. Morgan, M. E. Fox, and J. V. Watson. 1990. Mitoxantrone-DNA binding and the induction of topoisomerase II associated DNA damage in multi-drug resistant small cell lung cancer cells. *Biochem. Pharmacol.* 40:2069–2078.

Smith, P. J., H. R. Sykes, M. E. Fox, and I. J. Furlong. 1992. Subcellular distribution of the anticancer drug mitoxantrone in human and drug-resistance murine cells analyzed by flow cytometry and confocal microscopy and its relationship to the induction of DNA damage. *Cancer Res.* 52:4000–4008.

Udenfreid, S. 1965. Fluorescent analysis in biology and medicine. Mir, Moscow.

Wallace, R. E., D. Lindh, and F. E. Durr. 1987. Development of resistance and characteristics of human colon carcinoma subline resistant to mitoxantrone in vitro. *Cancer Invest.* 5:417–428.

Wang, J. C. 1996. DNA topoisomerases. *Annu. Rev. Biochem.* 65: 635–692.

Wolf, C. R., J. S. Macpherson, and J. F. Smyth. 1986. Evidence for the metabolism of mitoxantrone by microsomal glutathione transferases and 3-methylcholanthrene inducible glucuronosyl transferases. *Biochem. Pharmacol.* 35:1577–1581.

Zini, N., S. Santi, A. Ognibene, A. Bavelloni, L. M. Neri, A. Valmori, E. Mariani, C. Negri, G. C. B. Astaldi-Ricotti, and N. M. Maraldi. 1994. Discrete localization of different DNA topoisomerases in HeLa and K562 cell nuclei and subnuclear fractions. *Exp. Cell Res.* 210:336–348.